Future Medicinal Chemistry

Fluorinated MRI contrast agents and their versatile applications in the biomedical field

Journal:	*Future Medicinal Chemistry*
Manuscript ID	Draft
Manuscript Type:	Review
Keywords:	Chemical probes, NMR, Drug development

Version: 6th December 2017

Article Body Template

PLEASE DO NOT INCLUDE ANY IDENTIFYING INFORMATION IN THE MAIN BODY OF THE MANUSCRIPT

- **Abstract:**

Medical imaging is a dynamic area of research and the elaboration of more efficient contrast agents (CAs) constitutes a major objective. Those agents need to be improved to optimize the detection of affected tissues while decreasing the injected quantity of agents. Magnetic Resonance Imaging (MRI) has been recognized as one of the most applied medical imaging technique in clinical practice. However, the presence of background signal coming from water protons in surrounding tissues makes the visualization of local contrast agents difficult. Fluorine was then introduced as a reliable perspective thanks to its magnetic properties relatively close to those of protons. In this review, we aim to give an overall description of fluorine incorporation in contrast agents for magnetic resonance imaging.

- **Lay abstract:** N/A
- **Graphical abstract:** N/A
- **Video abstract:** N/A

- **Keywords:**

medical imaging; MRI; contrast agents; gadolinium complexes; paramagnetic compounds; fluorine; PFC; cell tracking; drug delivery

- **Main body of text:**

Introduction

Version: 6th December 2017

Article Body Template

Over decades, medical imaging has become an expanding field since the X-rays discovery by Wilhelm Röntgen in 1895. Those techniques enable to visualize inside the human body without the use of surgery. It is then possible to establish diagnosis but also to follow or treat some pathologies and diseases like atherosclerosis [1]–[5], cardiovascular or heart diseases [6]–[11], Alzheimer disease [12]–[16], tumors and cancers [17]–[20], etc. thanks to tissue three-dimensional reconstitutions or organ evolution monitoring through time.

The obtained information can then be treated to learn more either on the organ morphology or on its metabolism and functioning. Structural/anatomical imaging such as computed tomography (CT), magnetic resonance imaging (MRI) or ultrasound (US) are characterized by a relatively high spatial resolution but also by an overall lack of sensitivity. Functional imaging, such as optical imaging (OI), positron-emission tomography (PET) and single-photon-emission tomography (SPECT), are distinguished by a good detection of molecular and cellular changes of diseases but a poor spatial resolution.

Multimodal imaging [6], [21]–[25] is a relatively new technique able to provide more accurate diagnosis thanks to the combination of the different imaging techniques strengths meanwhile excluding their weaknesses. It is then possible to associate a poor spatial resolution technique such as SPECT or OI with a high spatial resolution but less sensitive one like MRI or CT scan.

Modality	Spatial resolution	Depth	Advantages	Inconvenient
CT	50-200 mm	No limit	High spatial resolution	Radiation, poor tissue imaging
MRI	0.01-0.1 mm	No limit	High spatial resolution, excellent signal in soft	Targeted imaging tracer availability, low sensitivity

			tissues, no ionizing radiation	
US	50-500 mm	mm-cm	Relatively good spatial and temporal resolution, safety	Low sensitivity
OI	1-5 mm	mm	High sensitivity, no radiation exposure, high throughput	Poor tissue penetration, low resolution
PET / SPECT	0.5-2 mm	No limit	Good sensitivity, dynamic	Targeted imaging tracer availability, radiation, low spatial resolution

MRI, among all the imaging methods, presents the propitious combination of high penetration depth, excellent soft tissue differentiation, high spatial resolution and safety thanks to the lack of ionizing radiation [1]. It is then recognized as one of the most applied medical imaging technique in clinical practice.

Conventional magnetic resonance techniques are based on the signal detection from mobile protons of water molecules. The image contrast depends on the protons concentration in the tissues and on their longitudinal and transversal relaxation times T_1 and T_2. Those tissues relaxation times can be modified by the use of contrast agents (CAs) [22] able to decrease either the longitudinal relaxation time - usually paramagnetic gadolinium (Gd^{3+}) complexes generating a positive contrast, or the transversal relaxation time - superparamagnetic CAs also known as negative CAs, mostly iron oxide nanoparticles. The image

contrast between targeted tissues and background signal is thus enhanced which allows to provide further information about tissues morphology and physiological processes.

Most of the clinically available MRI CAs are based on gadolinium ion (Gd^{3+}) because of its paramagnetic properties provided by its seven unpaired electrons, its long electronic relaxation time (around 10^{-9}s) and its large magnetic moment (7,9 BM) [23], [26]–[28]. Nevertheless, Gd^{3+} has a high toxicity for the tissues in its free state. Indeed, gadolinium ionic radius (~1.08 Å) can be compared to calcium ionic radius (~1.14 Å) so that Gd^{3+} can replace calcium ions in the tissues. To counter that toxicity and avoid its release in the tissues, gadolinium must form stable complexes with organic ligands to be carried out through the renal system and then be excreted. Gadolinium-based contrast agents (GBCAs) can be divided into 2 different classes regarding their chemical structure: linear and macrocyclic ligands. Those classes are distinguished by their thermodynamic and kinetic inertness [29] and their tendency to release gadolinium *in vivo* leading to nephrogenic systemic fibrosis (NSF), a rare and serious disease that causes severe fibrosis of skin and internal organs [30]. Whereas macrocyclic GBCAs form a rigid cage with a preorganized cavity for the gadolinium ion as established by J.M Lehn [31], linear ligands form more flexible cages around Gd^{3+} and do not envelop it entirely. Macrocyclic GBCAs are characterized by a high stability and are basically inert under physiological conditions while linear GBCAs are less stable and associated with NSF [19].

Linear GBCAs

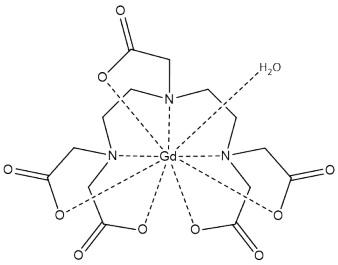

MAGNEVIST ® (Gd-DTPA)

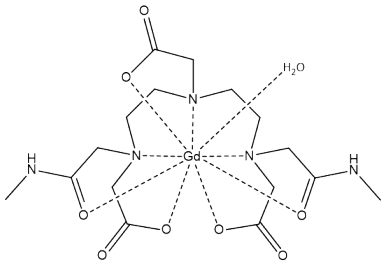

OMNISCAN ® (Gd(DTPA-BMA))

Macrocyclic GBCAs

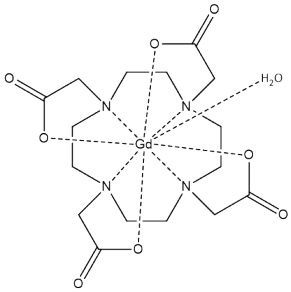

DOTAREM ® (Gd-DOTA)

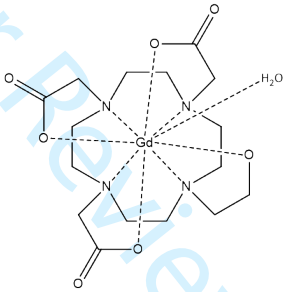

Prohance ® (Gd(HP-DO3A))

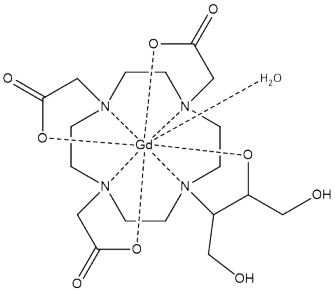

Gadovist ® (Gd(DO3A-butrol))

According to several reports published by Radbruch *et al.* [32] and Kanda *et al.* [33], GBCAs administration could engender gadolinium accumulation in the brain, especially (but not only) in dentate nucleus (DN) and globus pallidus (GP). However, studies have shown that no significant signal intensity increase (SI) was observable after serial injections of macrocyclic GBCAs while a significative SI increase was noticed after several previous linear GBCAs injections. Moreover, a substantially larger dose of CA per MR imaging session was injected in the macrocyclic GBCAs group compared to the linear GBCAs one. Also, as reported by Kanda *et al.* in 2015 [34], tissues concentrations of elemental gadolinium resulting from linear GBCAs were between 2.5 and 4 times higher to equivalent intravenous macrocyclic GBCAs doses [35]–[43].

One major drawback for the analysis of MRI images is the nonlinear relation between SI and CAs concentration coming from the magnetic inhomogeneities, but also from their indirect detection via their effect on water protons relaxation times. Another important drawback is the presence of the background signal resulting from water protons in the surrounding tissues. It is thus sometimes difficult to visualize the precise localization of the GBCAs. Recent alternatives have been formulated such as the use of heteronuclei to counter these complications. In this review, we will focus on the fluorine nucleus incorporation in MRI probes for their use in ^{19}F MRI.

Fluorine in medical imaging

Fluorine-19 was first isolated by Professor Henri Moissan in 1886 for which he received, in 1906, the Nobel Prize in chemistry. It is well-known that carbon-fluorine bond is one of the strongest single bond in organic chemistry [44]–[46] resulting from the high electronegativity of fluorine atom, leading to highly polarized C-F bond in which the electron density is shifted towards fluorine.

The fluorine-19 (^{19}F) nucleus is characterized by a natural abundance of 100 %, a nuclear spin I = ½ and a large chemical shift range (> 300 ppm). ^{19}F is the only natural stable fluorine isotope and its NMR sensitivity is of 83.4 % compared to the proton sensitivity. Its gyromagnetic ratio of 40.08 MHzT^{-1} is slightly lower than that of ^{1}H. Fluorine has 7 outer-shell electrons leading to strong chemical shift effects [47]. Compared to the ^{1}H nucleus, fluorine MRI signal-to-noise ratio (SNR) is of about 89 % which makes it a good alternative to proton MRI.

Physiological concentrations of fluorine atoms are below the detection limit of magnetic resonance technique. Moreover, fluorine is also present at higher concentrations in bones and teeth but in solid

form resulting in extremely short transverse relaxation time (T_2) which makes the signal invisible in conventional MRI. The administration of exogenous fluorine-containing contrast medium can then be monitored without any interference from the intrinsic background signal thanks to the use of a channel for the fluorine atoms. Information from the ^{19}F channel can then be combined with the anatomical information obtained by the ^{1}H channel leading to $^{1}H/^{19}F$ MR imaging which is not hindered by intrinsic variations in the tissues background intensity [47].

The administration of fluorinated drugs or contrast agents can be performed intravenously, orally, intratumorally or through inhalation. When fluorine is incorporated in drugs, it modifies the drugs original chemical properties (the drugs are made more lipophilic), biological activity as well as biodistribution.

The design of ^{19}F MRI probes needs to be elaborated with caution because of the conflict between the need of several chemically equivalent fluorine atoms and the hydrophobicity resulting from those fluorines. A too small amount of ^{19}F nuclei causes an undetectable signal whereas too many ^{19}F nuclei induces a low solubility in aqueous solution [48]. Moreover, a critical limiting factor for ^{19}F MRI is the long longitudinal relaxation time T_1 of fluorine when it is incorporated in small molecules. As a consequence, ^{19}F MRI images require long acquisition times. To solve this problem, different types of fluorinated CAs have been developed.

As reviewed by Tirotta *et al* in 2015 [49], fluorinated tracers can be divided in several chemical classes such as molecular tracers (perfluorinated organic molecules associated or not to a paramagnetic ion), polymeric tracers like linear perfluoropolyethers, statistical or block fluorinated copolymers, (hyper)branched fluorinated compounds such as dendrimers-based agents, fluorinated metallic

nanoparticles and multimodal imaging agents. ^{19}F MRI relying on the use of fluorinated tracers is applied in numerous biomedical applications such as multimodal imaging, drug delivery, cell tracking, etc.

Fluorinated probes

Perfluorocarbons

Perfluorocarbons (PFC) are organofluorine compounds from which all or most of the hydrogen atoms have been replaced by fluorine atoms. Those compounds have unique properties thanks to the exceptionally strong carbon-fluorine covalent bond and the strong electron withdrawing effect of fluorine atoms. PFCs have the particularity to be both lipophobic and hydrophobic and are characterized by high oxygen solubility, inertness and low surface tension [50]. PFCs can be divided in two types: the small chain PFCs are gases while larger chain PFCs are liquids. Because gaseous PFCs cannot be injected intravenously without risking embolism, liquids PFCs are preferred for medical practice. Moreover, only small amounts of PFCs can be injected in the bloodstream because of their low solubility in water, biological fats and lipids. After being injected into the bloodstream, PFCs can passively diffuse into the blood, bind to plasma lipids and be carried out to the lung where they are mostly eliminated by expiration. However, most of the medical applications consist in the administration of PFCs in larger quantity as a PFC-in-water emulsion, where the fluorinated probes concentration can be increased.

Those liquid PFCs such as perfluoropentane (PFP), perfluorohexane (PFH), perfluoro-15-crown-5-ether (PFCE), etc. are well-documented and turned to be safe, biocompatible, physiologically inactive, non-carcinogen, non-mutagen and non-teratogen except for perfluorooctane sulfonate (PFOS) and

perfluorooctanoic acid (PFOA) [51], [52]. As PFCs contain numerous fluorine atoms, they allow to enhance the SNR, decreasing the scanning time for high-resolution images acquisition [53].

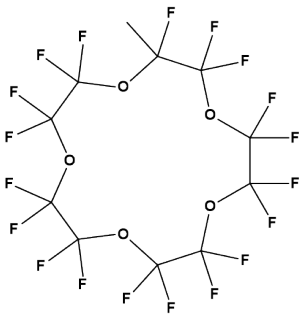

Perfluoro-15-crown-5 ether (PFCE)

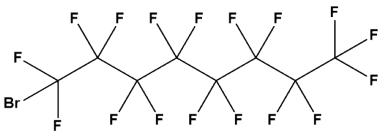

Perfluorooctyl bromide (PFOB)

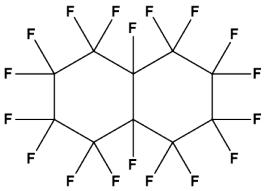

Perfluorodecalin (PFD)

In perfluorocarbonated nanoemulsions, liquids PFC cores, corresponding to 98% of the total nanoparticle volume, are encapsulated in a lipid monolayer able to be functionalized to contain different imaging or therapeutic agents. PFCs (figure 3) are incorporated into the lipid monolayer core while targeting agents and other payloads can be linked to the particles surface, inserted in the core or in the lipid membrane layer [54] (figure 3).

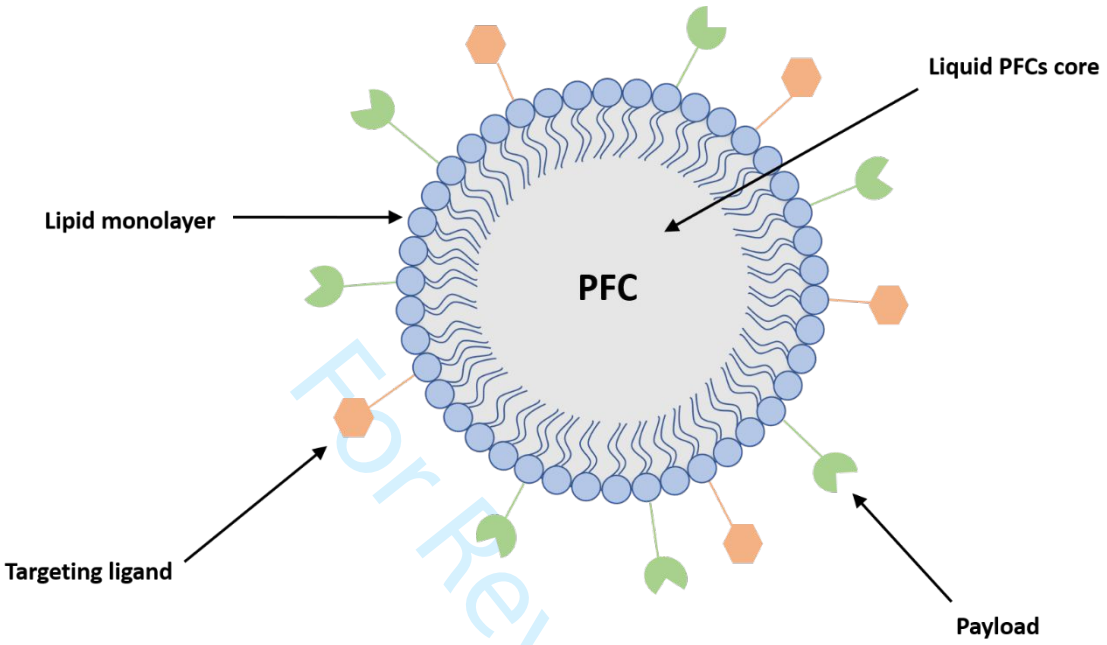

Several scientific groups [55]–[57], have developed a stable, biocompatible and water dispersible nanoprobe called FLAME (FLuorine Accumulated silica nanoparticle for MRI contrast Enhancement) composed of a liquid PFCs core surrounded by a silica shell. Matsushita *et al.* [55] have reported the modification of FLAMEs to enhance permeability and retention (EPR) effect and boost their accumulation in tumorous tissues instead of being immediately eliminated from the body. FLAMEs (figure 4) were modified by adding polyethylene glycol (PEG), reducing the uptake by the macrophages and making possible the visualization of the tumor area by ^{19}F MRI, superimposed on ^{1}H MRI anatomical images. While FLAME-PEG accumulates both in tumor sites and liver, non-PEGylated FLAMEs are only detected in the liver, showing their direct elimination by the reticuloendothelial system (RES).

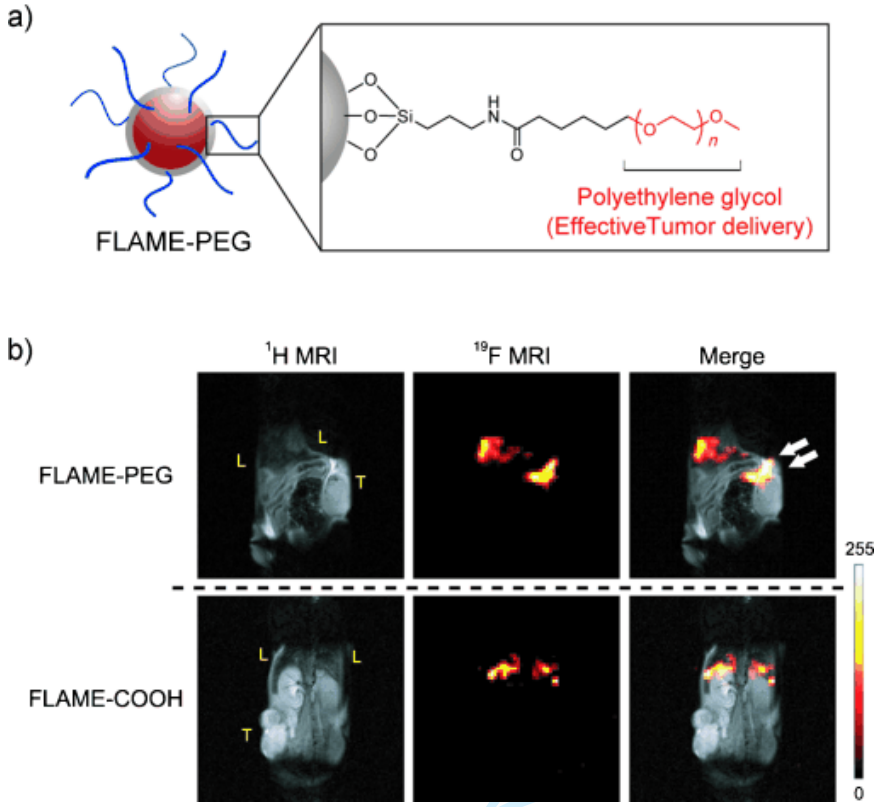

As reported in the literature by Nieuwoudt *et al.* [58] and Krafft *et al*. [59], PFC-loaded nanoparticles half-life in the blood and the RES depends on their size and coating properties. It is ranged from 3 days to more than 60 days depending on species and PFC compounds.

Fluorinated nanoparticles (silica, gold)

The association of inorganic nanoparticles and fluorinated ligands turned out to be an innovative approach in ^{19}F MR imaging providing several advantages such as the facility to introduce additional functionalities for dual or molecular imaging and the diminution of the systems size compared to the nanoemulsions. Boccalon *et al.* [60] have reported the synthesis of a dual fluorescence/^{19}F MRI probe composed of fluorinated amphiphilic ligands, protecting gold nanoparticles, to which several ligand-dyes

can be introduced. In 2015, Pengo *et al.* [61] have reviewed an overall description of different fluorinated gold nanoparticles as well as their properties and possible applications.

Bouchoucha *et al.* [62] have also reported fluorinated silica mesoporous nanoparticles able to be used as theranostic materials for dual MR imaging. Those mesoporous nanoparticles contain pores with diameters ranging from 2 to 50 nm, where drugs can be encapsulated. They can thus behave as drug delivery agents.

Fluorinated dendrimers

Dendrimers are organized tree-like molecules with nanometer-scale dimensions. They are usually spherical and constituted of a central core from which symmetrical branches (dendrons) are leaving. In ^{19}F MRI research field, dendrimers are appreciated thanks to their ability to incorporate multiple chemically equivalent fluorines in one molecule. In 2013, Y. B. Yu [63] has reported fluorinated bifunctional dendrimers composed of a fluorocarbon dendron, ^{19}F signal emitter and a hydrophilic one which is essential to enhance the water solubility of multi-fluorinated molecules. One of the first molecule reported is the 19FIT-27, containing 27 chemically identical fluorine atoms resulting in a single and sharp ^{19}F signal both *in vitro* and *in vivo* and characterized by a high water solubility. In 2015, Hernández-Ainsa *et al*. [64] have published a review on fluorinated dendrimers in which fluorines were incorporated in the periphery of dendrimers via covalent or ionic bonds. In 2017, Liu *et al.* [65] have developed fluorinated self-assembled “Janus” dendrimers. Those dendrimers are composed of two dendrimeric parts, each one presenting different functionalities. The hydrophobic head was constituted of fluorinated benzyl group with 12 symmetric fluorine atoms whereas hydrophilic tails were composed

of monodispersed oligoethylene glycol units. Upon drugs are co-assembled to the probe, marked changes in the SI were observed by ^{19}F NMR spectroscopy.

Fluorinated polymers

Some of the previously cited PFCs are fluorinated polymers such as perfluoropolyethers (PFPE). Linear perfluorinated polymers mixtures turned out to be used in a large scale for ^{19}F MRI cell labelling despite the fact that they are not soluble in water and require the association of hydrophilic segments or their incorporation in emulsions. Due to the large size of the nanoemulsions formed with perfluorinated polymers, leading to extended retention times, partially-fluorinated polymers (PFPs) have also been under investigation as alternative ^{19}F MRI agents [66].

Polymeric nanoparticles have been fully investigated over years because of their long blood circulation time and accumulation in diseased tissues, via EPR effect, making them appropriated, for example, as drug-delivery systems.

In 2014, Rolfe *et al.* [67] have developed polymeric nanoparticles for multimodal imaging combining the high-resolution ^{19}F/^{1}H MRI with the sensitive and versatile fluorescence imaging for *in vivo* tumors detection. This nanomedicine material was synthesized with excellent control over the hyperbranched structure allowing the *in vivo* distribution visualization. Ogawa *et al.* [68] have reported that atom-transfer radical polymerization of fluorinated compounds on a dendritic macroinitiator (PAMAM-Br) is a favorable approach to synthesize fluorinated polymer nanoparticles as a new type of highly sensitive ^{19}F MRI probe. Srinivas *et al.* [69] have developed polymer-encapsulated PFCs based on polylactic-co-glycolic acid. Those particles have demonstrated potential in simultaneous imaging of distinct cell

populations as well as labeling primary human dendritic cells subsets. More recently, Constantinides *et al.* [70] have proposed the use of new, functional, biodegradable and biocompatible natural or synthetic polymers blend scaffolds for ^{19}F MRI/MRS.

Paramagnetic fluorinated probes

Introduction

Among the numerous advantages of fluorine use in medical field, its long T_1 (ranging from 0.5 to 3 s for small diamagnetic compounds) has been so far, a critical limiting factor for the small fluorinated CAs because of the necessity to wait long repetition times and scan times. Scientists have solved this problem by combining paramagnetic or superparamagnetic agents to fluorinated probes. Their ability to enhance relaxation rates of nearby nuclei shortens the T_1 relaxation times of ^{19}F nuclei leading to record more scans within a timeframe and consequently to a better SNR. However, relaxing agents can also induce a T_2 decrease which can lead, in some cases, to a severe line broadening and absence of significant signal [49], [71], [72].

Paramagnetic PFC

Neubauer *et al*. [73] have reported gadolinium grafting to the outer surface of PFC nanoemulsion droplets leading to a decrease of T_1 when the nanoparticles were targeted to fibrin clots *in vitro*. However, distance lengthening between fluorine atoms and paramagnetic center restrains the relaxation rate enhancement. An alternative to this problem could be the introduction of paramagnetic metal ions as payloads into the nanoemulsion droplets to attain short spin-lattice relaxation time (T_1) and enhance targeted MR molecular imaging.

In 2014, de Vries *et al.* [74] studied relaxometry on gadolinium-functionalized PFC nanoparticles. They reported the influence of three different gadolinium-based molecules, hooked to the lipid monolayer, on water proton and fluorine relaxation rates. It appears that at current clinical field (1.5 – 3.0 T), favorable ^{19}F relaxivity values are observed while gadolinium is a disadvantage at higher field (6.3 – 9.4T) since it does not increase $^{19F}R_1$ but increases significantly the $^{19F}R_2$.

Hitchens *et al.* [75] have reported in 2015 a proof-of-concept of the effects of superparamagnetic iron oxide (SPIO) contrast agents on the PFCs properties commonly used in cell labeling.

Even though gadolinium chelates, with a high magnetic moment, are used as clinical ^{1}H MRI contrast agent, Kislukhin *et al.* [76] have based their research on FETRIS, a "ferric *tris*-diketonate", nanoemulsions using PFPE-based β-diketones (FDKs) as chelates to ferric metal ion (Fe^{3+}). In their study, they developed the idea that ferric ion seems to be better suited as T_1 enhancer for PFCs since gadolinium or lanthanide ions provoke large line broadening, becoming principally ^{19}F T_2 contrast agents. They also demonstrated that FDK (fluorinated β-diketones) are able to incorporate considerable amounts of paramagnetic metal ions into their fluorous phase, showing efficiency to irreversibly extract ferric ions from an aqueous solution into the fluorous phase. In this study, Kislukhin proved that gadolinium and ferric ions are respectively T_1 and T_2 agents for ^{1}H MRI but inversely for ^{19}F MRI.

Lanthanide-based fluorinated contrast agents

In ^{1}H MRI, paramagnetic chelates tend to be more appreciated than superparamagnetic compounds thanks to their ability to highlight the contrast of the accumulation zones. Fluorinated probes for *in vivo*

^{19}F MRI are most commonly associated with paramagnetic ions such as lanthanide ions (Gd^{3+}, Eu^{3+}, Dy^{3+}, Tm^{3+}, Er^{3+}, Ho^{3+} and Tb^{3+}) or ferric ion (Fe^{3+}) [76], …

Senanayake *et al.* [77] have reported a controllable approach consisting on positioning the ^{19}F nucleus at a fixed distance from the paramagnetic center, ideally in the range 4.5 and 7.5 Å in order to sufficiently shorten ^{19}F T_1 without dramatically shortening T_2 and decreasing the probe sensitivity.

Schmid *et al*. [78] have presented two concepts of paramagnetic relaxation enhancement (PRE) to increase relaxation rates. The first PRE studied is the intermolecular interaction between paramagnetic ion (gadolinium or lanthanide ion) and fluorine atoms. The second is the intramolecular PRE by interaction between lanthanide ion and fluorine within a single molecule. They were able to show a significative increase (factor 27) in the ^{19}F SNR for intramolecular PRE and the best results were achieved on agents containing gadolinium or dysprosium.

In 2010, Chalmers *et al.* [79] have reported the design and synthesis of paramagnetic fluorine-labelled lanthanide complexes as probes for ^{19}F MR imaging. Those dual-functional probes were composed of a macrocyclic complex of lanthanide (III) ion and a fluorinated group carefully positioned between 5 to 7 Å from the paramagnetic center. The effect of several paramagnetic ions (Tm, Er, Ho and Tb) was evaluated and an enhancement of the longitudinal relaxation rates was observed allowing faster acquisitions of data in a given time lapse and thus a signal intensity enhancement in hybrid $^{1}H/^{19}F$ MRI.

De Luca *et al.* [80] have studied in 2014 a new type of fluorinated probe composed of numerous fluorine atoms, CF_3 groups, linked to lanthanide (Tb, Dy, Ho) complexes and a biocompatible vector, chitosan. They have engineered medium molecular weighted molecules in which fluorine atoms are between 6 and 6.5 Å away from the paramagnetic center. This material do not have tendency to clear rapidly from

the body since the diffusion into the extravascular media is delayed, allowing the visualization of the fluorinated probe in MRI.

In 2015, Davies *et al.* [81] have reported the strong bidentate binding between an ethoxy-fluorinated isophthalic acid derivative and a binuclear lanthanide complex. This binding results in a large enhancement of the ^{19}F MRI relaxation rates, especially at physiologically pH range, making this probe relevant as ^{19}F MRI contrast agents.

Applications in medical imaging

Chemical exchange saturation transfer (CEST) agents

Chemical exchange saturation transfer (CEST) is a powerful sensitivity enhancement mechanism in which it is possible to visualize low concentration of solutes through water signal [82]. This approach is based on the selective saturation of exchangeable protons of endogenous or exogenous molecules by using a specific radiofrequency (RF) pulse. Once solutes protons are saturated, they transfer their saturation to protons of the bulk water, resulting in a decrease of the water signal.

It has been reported by Schmieder *et al*. [83] that fluorine-rich PFC nanoparticles can be used as a quantitative reference to normalize and characterize CEST but also multi-ion chemical exchange saturation transfer (miCEST) [84]. Lanthanide-based contrast agents (paraCEST) were developed to shift the resonances of exchangeable protons such as NH, OH or bound water. Cakić *et al.* [85] have demonstrated the potential of a multicontrast platform as paraCEST or ^{19}F MRI contrast agent. By combining those modalities, the agent, able to chelate a paramagnetic ion (Gd^{3+}, Eu^{3+} or Tb^{3+}), can be

observed in ^{1}H T_1-weighted, ^{1}H CEST and ^{19}F MR images. Differences have been noted between the three metal ion complexes showing that GdL and EuL complexes can be respectively used for ^{1}H T_1-weighted and ^{19}F MRI, or as a ^{1}H CEST and ^{19}F MRI agent.

In 2017, Peng *et al.* [86] have developed a class of fluorinated chelators with multiple symmetrical fluorine atoms as new ^{19}F ion-CEST imaging probes. When metal ions are chelated by the EDTA or DTPA derivatives, fluorine electron environment changes and induces a ^{19}F NMR response such as chemical shift changes or line broadening. A new peak can then be observed on the ^{19}F NMR spectra of chelators. It is then possible to use a RF pulse to saturate the "new" peak from the metal ion-bound chelators and detect the saturation transfer to the "free" chelators. In fact, metal ions are involved in a lot of biological processes which are intensively studied by scientists. The monitoring of their presence or their local concentration quantification turned out to be significant for their understanding. Peng *et al.* [86] have developed new ^{19}F CEST imaging probes and have applied them to sensitively and selectively detect metal ions. Compared to the known fluorinated metal ion chelators, theses probes were characterized by a strong and singlet ^{19}F NMR peak, are conveniently prepared on gram scales from commercially available chelators and are not sensitive to their environment such as differences of pH and temperature.

Smart ^{19}F -containing contrast agents

Fluorinated enzymes-responsive agents

Mizukami *et al*. [87], [88] have developed new ^{19}F MRI probes (figure 5) able to detect the caspase-3 protease activity, hallmark of apoptosis mechanisms [89]. Their studies are based on the PRE effect to

switch ON/OFF the probe MRI signals. Two fluorinated MRI probes, Gd-DOTA-DEVD-Tfb (Gd-DOTA = paramagnetic complex, DEVD = caspase substrate peptide, Tfb = para-trifluoromethoxybenzyl) and Gd-DOTA-DEVD-AFC (AFC = 7-amino-4-trifluoromethylcoumarin) have been reported to detect protease activity. The first agent is composed of a gadolinium complex, an enzyme substrate peptide and a ^{19}F-containing group. By the use of Gd^{3+} complexes, transversal relaxation time T_2 is shortened in ^{19}F NMR, attenuating the MRI signal in a broad peak. By the presence of caspase-3 enzyme, the peptide sequence DEVD is selectively cleaved on the C-terminal peptide bond, releasing the fluorinated group from the paramagnetic effect of gadolinium complexes and enhancing the ^{19}F MRI signal. The second developed probe consist in a new dual-functional probe able to detect protease activity by dual signal enhancement in both fluorescence and ^{19}F MRI. More recently, Yuan *et al.* [90], [91] designed ^{19}F MRI probes for the detection of caspase 3/7 or legumain activity in zebrafish. Akazawa *et al*. [57] have also reported the *enzyme-responsive* character of their probe relying on the "OFF"/"ON" switching strategy to detect caspase activity.

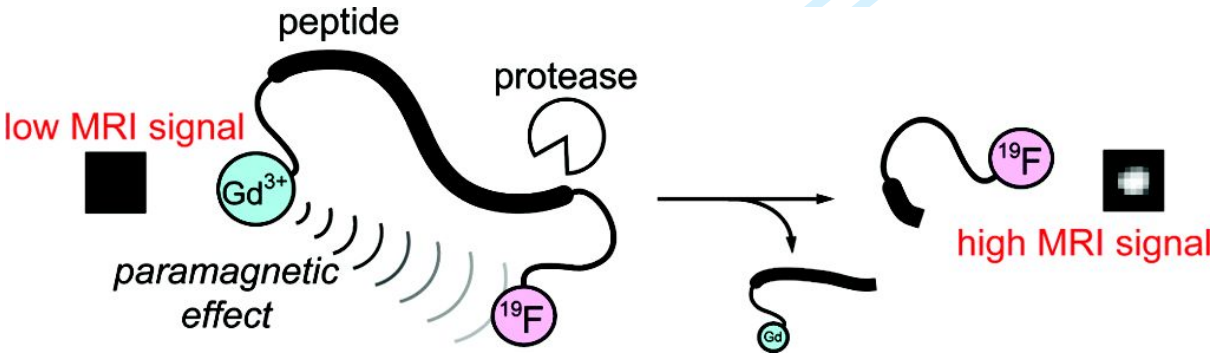

Fluorinated redox-responsive agents

In 2017, Basal *et al.* [48] have reported a new redox-active water soluble probe based on Europium ion, and twelve chemically equivalent fluorine nuclei, which is detectable *in vivo* before and after oxidation process by ^{1}H and ^{19}F MRI. The intramolecular fluorous interactions of the probe allow the formation of a cage-like structure modulating the interactions of water with europium according to the temperature. Their study relies on the difference between Eu^{II} and Eu^{III} ion respectively paramagnetic and diamagnetic [92]. Unlike Gd^{III} which is not redox-active *in vivo*, oxidation of Eu^{II} to Eu^{III} should remove quenching of ^{19}F signal. They have demonstrated that Europium-containing complexes act as T_1-shortening contrast agent for ^{1}H MRI when europium is in its +2 oxidation state and activate ^{19}F MRI probes in response to oxidation of Eu^{II} to Eu^{III}.

Fluorinated pH-responsive agents

It is well known that tumoral tissues differ from normal tissues in terms of pH. While the physiological pH is 7.4, the extracellular tumor environments is around pH 6.5. This difference allows then to target diseased tissues for diagnosis or drug delivery.

Oishi *et al*. [93] have developed a pH-sensitive PEGylated nanogel loaded with fluorinated molecules showing a significant ^{19}F MR signal despite the low fluorine concentration, phenomenon in response to the extracellular pH of tumor environments. More recently, Wang *et al*. [94] reported the synthesis of pH-responsive star polymer nanoparticles as potential ^{19}F MRI contrast agents in the diagnosis of cancer tissues. The three-dimensional branched structure, also known as star structure, allows the fluorine to be distant enough to maintain high molecular mobility, generating a strong ^{19}F MRI signal. Moreover, star polymers enable a lot of post-modifications thanks to the numerous functional groups. This probe was able to change the ^{19}F MRI image intensity from alkaline to acidic medium (from pH 9 to 4). In the

recorded ^{19}F NMR spectra, they demonstrated the constant intensity and width of the fluorine peaks when pH is below 7.4 while above this pH, the same peak appears broader and less intense. This difference in behavior demonstrates the potential of fluorinated star polymers as CAs.

Fluorinated thermo-responsive agents

Another difference between tumoral and healthy tissues is their temperature. Indeed, tumor tissues have higher temperatures because of their higher activity and energy requirements [95]. It has been accepted that tumoral tissues have a global temperature of 42°C compared to 37°C for healthy tissues. In 2009, Langereis *et al*. [96] have reported a temperature-sensitive CA for both ^{1}H CEST and ^{19}F MRI as a potential nanocarrier for drug delivery. The principle is the combination of liposomes containing both chemical shift agents (for ^{1}H lipoCEST detection) and fluorinated compounds (for ^{19}F detection) with focused ultrasound to cause local hyperthermia leading to the release of the chemical shift agent and hence the appearance of a ^{19}F MRI signal. More recently, Iima *et al.* [95] have assayed the synthesis of thermally responsive lipid nano-emulsions (LNE) containing fluorine atoms, producing a tunable ^{19}F MR signal in response to thermal stimulus, changing solid oil into a liquid oil and releasing its content. Three high-melting-point neutral lipids were selected and compared regarding their behavior at several temperatures (25, 37 and 42°C).

Recently, in July 2018, Kolouchova *et al*. [97] have developed new biocompatible, temperature-responsive polymeric nanogels containing enough fluorine atoms to be imaged in ^{19}F MRI. Theses amphiphilic nanogels are composed of a hydrophilic biocompatible block (PHPMA or PMeOx block) and

a fluorinated thermo-responsive (PDFEA) block which can control the process of nanoparticle self-assembling upon its heating in aqueous solution. At body temperature, nanoparticles combine together and form a nanosized system while the system remain soluble as unimers at room temperature. They described for the first time self-assembled thermo-responsive polymer nanogels appropriated for ^{19}F MRI.

Drug Delivery

One of the major research field in medical chemistry is the ability to deliver drugs to diseased tissues without being spread on the entire body. This process is called “drug delivery” and relies on limiting the side effects of drugs by their encapsulation in nanocarriers such as micelles, liposomes, lipids monolayers, etc. [98]. Those liposome or micelle-based drug-delivery systems are principally based on the self-assembly of amphiphilic molecules allowing the encapsulation, the stabilization and the delivery of drugs in the appropriate tissues [65].

In tumor treatment, chemotherapy drugs, highly cytotoxic, are administrated to patients to kill cancer cells. However, it appears that those chemical drugs are not specific enough, attack normal cells and provoke serious side effects. Therefore, tumor-targeted drug-delivery systems have been developed to selectively deliver cytotoxic drugs to cancer cells exploiting the intrinsic physiological and biochemical properties of those cells [99]. Those delivery carriers are based on a “smart” linker which is stable during blood circulation but cleaved to release drugs as soon as it is in the tumor environment.

Seitz *et al.* [99] have described the design and the synthesis of two ^{19}F NMR probes to study the drug release in biological media. Those probes were composed of biotin (the tumor-targeting part), a linker and fluorotaxoid molecules for the visualization in ^{19}F NMR spectroscopy.

In 2016, Vu-Quang *et al.* [100] have developed a multimodal imaging and therapeutic platform by encapsulation of several molecules in polymer nanoparticles for dual-imaging. This probe was composed of doxorubicin (Dox) molecules, used in chemotherapy, an indocyanine green NIR (near-infrared) imaging agent as well as perfluorooctyl bromide (PFOB), a fluorinated molecule for ^{19}F MRI. This material was able to transport anti-cancer drugs making it a reliable drug-delivery system for chemotherapy.

Recently, Bo *et al*. [101] have developed a fluorinated dendritic ^{19}F MRI-detectable liposomal drug-delivery system allowing the non-covalent encapsulation of drugs and containing 81 chemically equivalent fluorine atoms linked to the liposomal membrane to give strong signal in ^{19}F MRI.

Cell tracking

Cell tracking turns out to be an interesting tool for the cellular therapy research domain where the objective is to stimulate the immune system in order to provoke an immune response and regenerate damaged tissues using stem cells [102].

As an alternative to iron oxide nanoparticles usually used, cyclic PFCE and linear PFPE can be employed to improve SNR as well as detectability in cell tracking field.

In 2005, Eric T Ahrens *et al.* [103] were one of the first to report MRI technology for *in vivo* cell tracking using a PFC tracer agent. Unlike methods based on metal-ion CAs, this cell tracking technique based on

PFPE is very selective to labeled cells. Cells are firstly labeled *ex vivo* with PFPE agents, then administrated and tracked by ^{19}F MRI. They focused their study on dendritic cells, efficient antigen-presenting cells able to initiate an immune response.

Kaneda *et al.* [54] have described a fluorine nanoparticles MR molecular imaging procedure by employing a preparation of PFCE nanoparticles to charge dendritic immune cells without loss of viability. They also demonstrated the possibility to track cells at high magnetic field (11.7 T) after local and systemic injection of fluorine agents leading to the signal detection from the targeted cells. In 2010, Helfer *et al*. [104] have reported the ability to image PFPE-labeled human dendritic cells once injected without background from the host, making the interpretation easier when ^{19}F images are superimposed with conventional ^{1}H images.

Ahrens *et al.* [105], [106] have developed, few years later, PFC nanoemulsions for detection of immune-therapeutic dendritic cells delivered to colorectal adenocarcinoma patients. This PFC tracer agent has undergone phase I clinical trial for ^{19}F MRI cell tracking applications proving their efficacity in medical applications. In 2015, Gaudet *et al*. [107] have demonstrated the ability to use ^{19}F MRI cell tracking to detect and measure the number of transplanted stem cells with excellent correlation to *in vivo* quantification using Voxel Tracker software as previously reported by Srinivas *et al.* [108].

Several studies have confirmed that ^{19}F MRI could be an appropriated method to track macrophages in a large scale of diseases such as arthritis [109], cancer [110], [111], pulmonary inflammation [112], cardiovascular inflammation [113], [114] or transplantation rejection [115]–[117].

In 2017, Huyn Shin *et al*. [118] were the first to develop a ^{19}F MRI and ^{18}F-FDG-PET bimodal probe able to provide complementary information to comprehensively monitor the tumor microenvironment. They

have shown that this probe was able to help in the characterization of tumors and prediction of tumor development thanks to the ability to track tumor-associated macrophages (TAMs), cells associated with tumor growth and metastasis.

The same year, Makela *et al*. [119] have evaluated and compared iron-based and fluorine-based MRI techniques to image TAMs in a breast cancer model. The outcomes of this study were the same spatial distributions of TAMs but also an underestimated cell density of TAMs for ^{19}F-based probes relying on its detection sensitivity which is much lower compared to iron oxides particles.

Several groups, Khurana *et al*. [120], Makela *et al.* [121] and Huyn Shin *et al.* [122], have also reported ^{19}F-based MRI cell tracking by using *in vivo* PFC-labelled nanoparticles to detect, quantify and track TAMs inside murine orthotopic breast cancer tumors and its associated metastasis or in mouse model of head and neck squamous cells carcinoma.

Fink *et al*. [123] have investigated the feasibility to use ^{19}F-PFC agent as an MRI cell labeling agent for the administration of peripheral blood mononuclear cells (PBMC)-based cancer vaccine. They were able to quantify the signal from ^{19}F-PFC-labeled PBMC at a depth of around 1 cm.

In 2015, Bo *et al.* [124] have reported a novel ^{19}F MRI/fluorescence dual-imaging agent containing 48 symmetrical fluorine atoms resulting in a single ^{19}F NMR signal and a better SNR for the detection of labelled cells. This probe was characterized by a high aqueous solubility, a high fluorine MRI sensitivity and a low toxicity. More recently, Moonshi *et al.* [66], have designed and synthesized a novel partially-fluorinated copolymer conjugated with a fluorescent dye for dual-imaging. Their copolymer is composed of a fluorinated monomer (PFPEMA) and a hydrophilic component (OEGMA) to confer water solubility.

This dual MR/fluorescence imaging agent allowed the *in vivo* detection of labelled cells throughout 7 days post-injection with distinct signal.

In the same research field, Peng *et al.* [125] have developed multifunctional paramagnetic fluorinated nanoemulsions containing 27 symmetrical fluorine atoms, characterized by a high paramagnetic relaxation enhancement, a single ^{19}F NMR signal, a high stability and biocompatibility. This versatile probe could be employed as a versatile platform for cell tracking.

Inflammation visualization

Inflammation processes are involved in a lot of diseases and are characterized by the accumulation of neutrophil granulocytes (nonspecific leukocytes) and monocytes (dendritic cells or macrophages) in the inflamed area. As the evolution of the inflammation is decisive for healing processes, it is important to monitor the inflammation response. For that, it is essential to track the previously cited implicated cells by labelling them with a contrast agent [126]. After being injected, fluorinated probes (usually PFC nanoemulsions) can be adducted by the circulating monocytes and carried out to inflammation sites where they are visualized by ^{19}F MRI.

In 2014, Jacoby *et al.* [127] have published their work on the *in vivo* visualization of inflammation using 3 different PFC molecules (PFOB, PFD, F44E) as alternative to PFCE which is associated with deposition in liver and spleen even after months. In their study, they have demonstrated that PFOB tends to be the best choice but can not compete entirely with PFCE. Indeed, its half-life is about 12 days compared to 250 for PFCE but its relative sensitivity does not exceed 37 %. Those results were confirmed by Colotti *et al*. [128] in their comparison study on the three commonly used PFC emulsions: PFPE, PFCE and PFOB.

PFPE was characterized by the shortest T_1 value but no information was given on its clearance rate, whereas PFCE was characterized by the highest R_2/R_1 ratio but remains in spleen and liver for a long time after injection. PFOB, as previously said, is the best-suited candidate for inflammation imaging because of its fast elimination rate.

In 2015, van Heeswijk *et al.* [129] reported a proof-of-principle study on the use of PFCs to visualize the inflammation in atherosclerotic plaques.

Tumor detection – tumor ablation

Moyer *et al.* [130], [131] and Hyun Shin *et al.* [132] have demonstrated the ability of PFCE to guide high intensity focused ultrasound (HIFU) ablation of tumors by tracking PFC nanoemulsions accumulation zone in a visible and quantifiable way as an alternative of PFC gases microbubbles. Indeed, although microbubbles could enhance HIFU ablation of tumors, they also generate unforeseen prefocal thermal delivery and skin burns. The PFCs nanodroplets turn out to be an option of choice to avoid those inconvenience.

Wu *et al.* [133] have reported in 2018 the intratumoral IT PFC nanoparticles administration for the MRI diagnosis of lung cancer in Vx2 rabbit model. In this study, multifunctional paramagnetic fluorocarbon nanoparticles (M-PFC NP) have shown high biocompatibility, ideal size, oxygen dissolving capacity and natural bioelimination. They reported that IT M-PFC NP slowly penetrated the Vx2 tumor for 12 hours and stayed for 72 hours.

Conclusion

Article Body Template

In this review, we have reported the importance of fluorinated MRI CAs. Because of the lack of sensitivity and the presence of background signal from intrinsic protons when para- or superparamagnetic agents are used in ^{1}H MRI, fluorine MRI appears to be a good alternative in the medical imaging field. The number of publications on ^{19}F MRI highlights the interest of scientists for the development of fluorinated probes to improve diagnosis and treatments of numerous diseases. We have described here several fluorinated probes among which fluorinated nanoparticles, dendrimers, polymers, paramagnetic complexes and perfluorocarbons which tend to be very appreciated by the scientists for their ability to be easily functionalized with paramagnetic complexes, targeting vectors and other payloads. A non-exhaustive list of applications for fluorine probes was described among which cell tracking, drug delivery, tumor ablation, biological or responsive smart agents.

- **Future Perspective:**

Fluorine magnetic resonance imaging was discovered in 1977, only four years after the development of proton MRI. Since the end of the 1990's, number of publications did not stop to increase, which makes easily predictable that fluorine will continue to be a dynamic research domain in imaging contrast agents. Among the cited fluorinated agents, PFCs nanoemulsions will continue to be under the scope of scientists thanks to their numerous advantages such as active targeting, protection of the liquid PFC core and their ability to incorporate different payloads. Paramagnetic fluorinated MRI contrast agents should also be developed more thoroughly way since the fluorine signal can be registered with a good sensibility in a relatively short acquisition time.

Version: 6th December 2017

Article Body Template

- **Executive Summary:**

Executive summary
Fluorine: • Natural abundance of 100%, nuclear spin ½ , only natural stable isotope, 83.4 % of proton sensitivity **Fluorinated probes:** • PFCs: hydrophobic and lipophobic, need to be incorporated in lipid monolayers as PFC nanoemulsions • Fluorinated nanoparticles: silica, gold fluorinated nanoparticles, smaller than nanoemulsions, can be functionalizable • Fluorinated dendrimers: possibility to incorporate numerous chemically equivalent fluorine atoms resulting in a single and sharp ^{19}F signal • Fluorinated polymers: polymeric nanoparticles highly sensitive in ^{19}F MRI, probes characterized by a long blood circulation time • Paramagnetic fluorinated probes: combination of (super)paramagnetic ion and fluorines allowing the decrease of fluorine relaxation times, bimodal contrast agents able to map anatomy and locate the fluorinated agent at the same time **Applications:** • CEST agents: possibility to visualize extremely low concentrated solutes by the decrease of the water bulk signal • "Smart" fluorinated agents: enzyme-, redox-, pH- and thermo-responsive agents changing their behavior according to an external stimulus • Drug delivery: applications in a lot of field, e.g. in chemotherapy where the cytotoxic drugs need to be encapsulated until they reach the targeted tumor cells • Cell tracking: usually PFCE or PFPE used to track cells like dendritic cells or macrophages • Inflammation visualization: perfluorocarbons used to track the inflammation process and inflamed areas

- Tumor detection and ablation: PFC used to visualize the accumulation zones (tumor) and guide the HIFU ablation of tumor

- **Figure legends:**

Figure 1 : Most common used commercially available gadolinium-based contrast agents

Figure 2: Chemical structure of some PFCs

Figure 3: Scheme of PFC nanoemulsions containing perfluorocarbonated core within a lipid monolayer on which payloads and targeting ligands can be linked.

Figure 4: *In vivo* distribution of FLAME at tumorous site. (a) Structure of PEGylated FLAME (b) *In vivo* images of the accumulation of FLAME PEGylated (FLAME-PEG) and non-PEGylated (FLAME-COOH) in tumor-bearing mice. The superimposition of ^{1}H and ^{19}F MRI images shows the difference between the distribution of FLAMEs in liver (L) and tumor (T) (Reprinted with permission from Matsushita H, Mizukami S, Sugihara F, Nakanishi Y, Yoshioka Y, Kikuchi K. Multifunctional Core–Shell Silica Nanoparticles for Highly Sensitive 19F Magnetic Resonance Imaging, Volume: 53, Issue: 4, Pages: 1008-1011, First published: 20 January 2014, DOI: (10.1002/anie.201308500) [55])

Figure 5 : Scheme of enzyme-responsive fluorinated agent to detect caspase-3 activity. (Reprinted with permission from Mizukami S, Takikawa R, Sugihara F *et al.* Paramagnetic relaxation-based ^{19}F MRI probe to detect protease activity. Copyright 2008 American Chemical Society [87])

- **Table Legends:**

Table 1: summary of most common used imaging techniques in clinical field [23], [25]

- **References:**

Papers of special note have been highlighted as:

* = of interest

** = of considerable interest

[1] Palekar RU, Jallouk AP, Lanza GM, Pan H, Wickline SA. Molecular imaging of atherosclerosis with nanoparticle-based fluorinated MRI contrast agents. *Nanomedicine (Lond.)* 10(11), 1817–1832 (2015).

[2] Hammad B, Evans NR, Rudd JHF, Tawakol A. Molecular imaging of atherosclerosis with integrated PET imaging. *J. Nucl. Cardiol.* 24(3), 938–943 (2017).

[3] Chueh JY, van der Marel K, Gounis MJ *et al.* Development of a high resolution MRI intracranial atherosclerosis imaging phantom. *J. Neurointervent. Surg.* 10(2), 143-149 (2018).

[4] Gepner AD, Young R, Delaney JA *et al.* Comparison of Carotid Plaque Score and Coronary Artery Calcium Score for Predicting Cardiovascular Disease Events : The Multi-Ethnic Study of Atherosclerosis. *J Am. Heart Assoc.* 6(2), pii: e005179 DOI: 10.1161/JAHA.116.005179 (2017).

[5] de Oliveira-Santos M, Castelo-Branco M, Silva R *et al.* Atherosclerotic plaque metabolism in high cardiovascular risk subjects - A subclinical atherosclerosis imaging study with ^{18} F-NaF PET-CT. *Atherosclerosis* 260, 41–46 (2017).

[6] Adenaw N, Salerno M. PET/MRI : Current state of the art and future potential for cardiovascular applications. *J. Nucl. Cardiol.* 20(6), 976–989 (2013).

[7] McRee CW, Mergo P, Parikh P, Pollak A, Shapiro BP. Modern advances in cardiovascular imaging: cardiac computed tomography and cardiovascular MRI in pericardial disease. *Future Cardiol*. 10(6), 769–779 (2014).

[8] Danad I, Szymonifka J, Twisk JWR *et al.* Diagnostic performance of cardiac imaging methods to diagnose ischaemia-causing coronary artery disease when directly compared with fractional flow reserve as a reference standard: a meta-analysis. *Eur. Heart J.* 38(13), 991–998 (2017).

[9] Krumm P, Mueller KAL, Klinge K *et al.* Cardiovascular magnetic resonance patterns of biopsy proven cardiac involvement in systemic sclerosis. *J. Cardiovasc. Magn. Reson.* 18(1), 70 DOI: 10.1186/s12968-016-0289-3 (2016).

[10] Catalano O, Moro G, Mori A *et al.* Cardiac Magnetic Resonance in Stable Coronary Artery Disease: Added Prognostic Value to Conventional Risk Profiling. *Biomed. Res. Int*. 2018, 2806148 DOI: 10.1155/2018/2806148 (2018).

[11] Mitchell C, Korcarz CE, Gepner AD *et al.* Ultrasound carotid plaque features, cardiovascular disease risk factors and events: The Multi-Ethnic Study of Atherosclerosis. *Atherosclerosis* 276, 195–202 (2018).

[12] Bort G, Catoen S, Borderies H *et al.* Gadolinium-based contrast agents targeted to amyloid aggregates for the early diagnosis of Alzheimer's disease by MRI. E*ur. J. Med. Chem.* 87, 843–861 (2014).

[13] Kehoe EG, McNulty JP, Mullins PG, Bokde AL. Advances in MRI biomarkers for the diagnosis of Alzheimer's disease. *Biomark. Med.* 8(9), 1151–1169 (2014).

[14] Ali R, Goubran M, Choudhri O, Zeineh MM. Seven-Tesla MRI and neuroimaging biomarkers for Alzheimer's disease. *Neurosurg. Focus* 39(5), E4 DOI: 10.3171/2015.9.FOCUS15326 (2015).

[15] Jack CR, Wiste HJ, Weigand SD *et al.* Defining imaging biomarker cut points for brain aging and Alzheimer's disease. *Alzheimers Dement.* 13(3), 205–216 (2017).

[16] Zhao Y, Raichle ME, Wen J *et al. In vivo* detection of microstructural correlates of brain pathology in preclinical and early Alzheimer Disease with magnetic resonance imaging. *Neuroimage.* 148, 296–304 (2017).

[17] Zhou Z, Lu ZR. Gadolinium-based contrast agents for magnetic resonance cancer imaging. *WIREs Nanomed. Nanobiotechnol.* 5(1), 1–18 (2013).

[18] Chandrasekharan P, Yang CT, Nasrallah FA, Tay HC, Chuang KH, Robins EG. Pharmacokinetics of Gd(DO3A-Lys) and MR imaging studies in an orthotopic U87MG glioma tumor model. *Contrast Media Mol. Imaging* 10(3), 237–244 (2015).

[19] Jeong Y, Na K. Synthesis of a gadolinium based-macrocyclic MRI contrast agent for effective cancer diagnosis. *Biomater. Res.* 22, 17 DOI: 10.1186/s40824-018-0127-9 (2018).

[20] Shazreen S, Saad FFA, Suhaimi SNM. PET-MRI Imaging of Cellular Trafficking of Lipid Metabolism and Its Association with Inflammatory and Genetic Markers in Breast Cancer. *Erciyes. Med. J.* 40(1), 1–7 (2018).

[21] Berkova Z, Jirak D, Zacharovova K *et al.* Gadolinium- and Manganite-Based Contrast Agents with Fluorescent Probes for Both Magnetic Resonance and Fluorescence Imaging of Pancreatic Islets: A Comparative Study. *ChemMedChem* 8(4), 614–621 (2013).

[22] Pierre VC, Allen MJ, Caravan P. Contrast agents for MRI: 30+ years and where are we going ? *J. Biol. Inog. Chem.* 19(2), 127–131 (2014).

[23] Zhang L, Liu R, Peng H *et al*. The Evolution of Gadolinium Based Contrast Agents; From Single-modality to Multi-modality. *Nanoscale* 8(20), 10491– 510 (2016).

[24] Truillet C, Bouziotis P, Tsoukalas C *et al.* Ultrasmall particles for Gd-MRI and ^{68}Ga-PET dual imaging. *Contrast Media Mol. Imaging* 10(4), 309–319 (2015).

[25] Burke BP, Cawthorne C, Archibald SJ. Multimodal nanoparticle imaging agents: design and applications. *Philos. Trans. A. Math. Phys. Eng. Sci.* 375(2107), DOI: 10.1098/rsta.2017.0261 (2017)

[26] Yang CT, Chandrasekharan P, He T *et al*. An intravascular MRI contrast agent based on Gd(DO3A-Lys) for tumor angiography. *Biomaterials* 35(1), 327–336 (2014).

[27] Rashid HU, Martines MAU, Jorge J *et al.* Cyclen-based Gd^{3+} complexes as MRI contrast agents: Relaxivity enhancement and ligand design. *Bioorg. Med. Chem.* 24(22), 5663–5684 (2016).

[28] Kaur J, Tsvetkova Y, Arroub K, Sahnoun S, Kiessling F, Mathur S. Synthesis, characterization, and relaxation studies of Gd-DO3A conjugate of chlorambucil as a potential theranostic agent. *Chem. Biol. Drug Des.* 89(2), 269–276 (2017).

[29] Frenzel T, Lengsfeld P, Schirmer H, Hütter J, Weinmann HJ. Stability of Gadolinium-Based Magnetic Resonance Imaging Contrast Agents in Human Serum at 37°C. *Invest. Radiol. 43(12)*, 817–828 (2008).

[30] Sieber MA, Lengsfeld P, Frenzel F *et al.* Preclinical investigation to compare different gadolinium-based contrast agents regarding their propensity to release gadolinium in vivo and to trigger

nephrogenic systemic fibrosis-like lesions. *Eur. Radiol.* 18(10), 2164–2173 (2008).

[31] Lehn JM. Supramolecular Chemistry - Scope and Perspectives: Molecules - Supermolecules - Molecular Devices. *Angew. Chem. Int. Ed. Eng*. 27(1), 89–112 (1988).

[32] Radbruch A, Weberling LD, Kieslich PJ *et al.* High-Signal Intensity in the Dentate Nucleus and Globus Pallidus on Unenhanced T1-Weighted Images Evaluation of the Macrocyclic Gadolinium-Based Contrast Agent Gadobutrol. *Invest. Radiol.* 50(12), 805–810 (2015).

[33] Kanda T, Fukusato T, Matsuda M *et al.* Gadolinium-based Contrast Agent Accumulates in the Brain Even in Subjects without Severe Renal Dysfunction: Evaluation of Autopsy Brain Specimens with Inductively Coupled Plasma Mass. *Radiology* 276(1), 228– 232 (2015).

[34] Kanda T, Osawa M, Oba H *et al*. High Signal Intensity in Dentate Nucleus on Unenhanced T1-weighted MR Images: Association with Linear versus Macrocyclic Gadolinium Chelate Administration. *Radiology* 275(3), 803–809 (2015).

[35] Kanda T, Oba H, Toyoda K, Furui S. Macrocyclic Gadolinium-Based Contrast Agents Do Not Cause Hyperintensity in the Dentate Nucleus. *AJNR Am. J. Neuroradiol.* 37(5), E41 DOI: 10.3174/ajnr.A4710 (2016).

[36] Radbruch A, Weberling LD, Kieslich PJ *et al.* Gadolinium Retention in the Dentate Nucleus and Globus Pallidus Is Dependent on the Class of Contrast Agent. *Radiology* 275(3), 783–791 (2015).

[37] Rogosnitzky M, Branch S. Gadolinium-based contrast agent toxicity: a review of known and proposed mechanisms. *Biometals. 29(3), 365–376* (2016).

[38] Lohrke J, Frisk AL, Frenzel T *et al.* Histology and Gadolinium Distribution in the Rodent Brain After the Administration of Cumulative High Doses of Linear and Macrocyclic Gadolinium-Based Contrast Agents. *Invest. Radiol.* 52(6), 324–333 (2017).

[39] McDonald RJ, McDonald JS, Dai D *et al.* Comparison of Gadolinium Concentrations within Multiple Rat Organs after Intravenous Administration of Linear versus Macrocyclic Gadolinium Chelates. *Radiology* 285(2), 536–545 (2017).

[40] Ramalho M, Ramalho J, Burke LM, Semelka RC. Gadolinium Retention and Toxicity—An Update. *Adv. Chronic Kidney Dis. 24(3)*, 138–146 (2017).

[41] Boyken J, Frenzel T, Lohrke J, Jost G, Pietsch H. Gadolinium Accumulation in the Deep Cerebellar Nuclei and Globus Pallidus After Exposure to Linear but Not Macrocyclic Gadolinium-Based Contrast Agents in a Retrospective Pig Study With High Similarity to Clinical Conditions. *Invest. Radiol.* 53(5), 278–285 (2018).

[42] Rasschaert M, Emerit A, Fretellier N *et al.* Gadolinium Retention, Brain T1 Hyperintensity, and Endogenous Metals: A Comparative Study of Macrocyclic Versus Linear Gadolinium Chelates in Renally Sensitized Rats. *Invest. Radiol.* 53(6), 328–337 (2018).

[43] E. Kanal. Gadolinium based contrast agents (GBCA): Safety overview after 3 decades of clinical experience. *Magn. Reson. Imaging* 34(10), 1341–1345 (2016).

[44] Bartusik D, Aebisher D. ^{19}F applications in drug development and imaging - a review. *Biomed. Pharmacother.* 68(6), 813–817 (2014).

[45] Park BK, Kitteringham NR, O'Neill P. Metabolism of fluorine-containing drugs. *Annu. Rev. Pharmacol. Toxicol.* 41(1), 443–470 (2001).

[46] O'Hagan D. Understanding organofluorine chemistry. An introduction to the C–F bond. *Chem. Soc. Rev.* 37(2), 308–319 (2008).

[47] Wolters M, Mohades SG, Hackeng TM, Post MJ, Kooi ME, Backes WH. Clinical perspectives of hybrid proton-fluorine magnetic resonance imaging and spectroscopy. *Invest. Radiol.* 48(5), 341–50 (2013).

[48] Basal LA, Bailey MD, Romero J *et al.* Fluorinated Eu^{II}-based multimodal contrast agent for temperature- and redox-responsive magnetic resonance imaging. *Chem. Sci*. 8(12), 8345–8350 (2017).

[49] Tirotta I, Dichiarante V, Pigliacelli C *et al.* ^{19}F Magnetic Resonance Imaging (MRI): From Design of Materials to Clinical Applications. *Chem. Rev.* 115(2), 1106 –1129 (2015).

[50] Díaz-López R, Tsapis N, Fattal E. Liquid Perfluorocarbons as Contrast Agents for Ultrasonography and ^{19}F -MRI. *Pharma. Res.* 27(1), 1–16 (2010).

[51] Chang ET, Adami HO, Boffetta P, Cole P, Starr TB, Mandel JS. A critical review of perfluorooctanoate and perfluorooctanesulfonate exposure and cancer risk in humans. *Crit. Rev. Toxicol.* 44(S1), 1–81 (2014).

[52] Kamendulis LM, Wu Q, Sandusky GE, Hocevar BA. Perfluorooctanoic acid exposure triggers oxidative stress in the mouse pancreas. *Toxicol. Rep.* 1, 513–521 (2014).

[53] Cosco D, Fattal E, Fresta M, Tsapis N. Perfluorocarbon-loaded micro and nanosystems for medical imaging: A state of the art. *J. Fluor. Chem.* 171, 18–26 (2015).

[54] Kaneda ME, Caruthers S, Lanza GM, Wickline SA. Perfluorocarbon Nanoemulsions for Quantitative Molecular Imaging and Targeted Therapeutics. *Ann. Biomed. Eng.* 37(10), 1922–1933 (2009).

[55] Matsushita H, Mizukami S, Sugihara F, Nakanishi Y, Yoshioka Y, Kikuchi K. Multifunctional Core–Shell Silica Nanoparticles for Highly Sensitive ^{19}F Magnetic Resonance Imaging. *Angew. Chem. Int. Ed. Eng.* 53(4), 1008–1011 (2014).

[56] Nakamura T, Sugihara F, Matsushita H, Yoshioka Y, Mizukami S, Kikuchi K. Mesoporous silica nanoparticles for ^{19}F resonance imaging, fluorescence imaging, and drug delivery. *Chem. Sci.* 6(3), 1986–1990 (2015).

[57] Azakawa K, Sugihara F, Nakamura T, Mizukami S, Kikuchi K. Highly Sensitive Detection of Caspase-3/7 Activity in Living Mice Using Enzyme-Responsive ^{19}F MRI Nanoprobes. *Bioconjug. Chem.* 29(5), 1720–1728 (2018).

[58] Nieuwoudt M, Engelbrecht GHC, Sentle L, Auer R, Kahn D, van der Merwe SW. Non-toxicity of IV Injected Perfluorocarbon Oxygen Carrier in an Animal Model of Liver Regeneration Following Surgical Injury. *Artif. Cells Blood Substit. Immobil. Biotechnol*. 37(3), 117–124 (2009).

[59] Krafft MP, Riess JG. Perfluorocarbons : Life Sciences and Biomedical Uses. *J. Polymer Science: Part A: Polymer chemistry* 45(7), 1185–1198 (2007).

[60] Boccalon M, Franchi P, Lucarini M *et al.* Gold nanoparticles protected by fluorinated ligands for ^{19}F MRI. *Chem. Commun. (Camb.)* 49(78), 8794–8796 (2013).

[61] Pengo P, Pasquato L. Gold nanoparticles protected by fluorinated ligands: Syntheses, properties and applications. *J. Fluor. Chem.* 177, 2–10 (2015).

[62] Bouchoucha M, van Heeswijk RB, Gossuin Y, Kleitz F, Fortin MA. Fluorinated Mesoporous Silica Nanoparticles for Binuclear Probes in ^{1}H and ^{19}F Magnetic Resonance Imaging. *Langmuir*. 33(40), 10531–10542 (2017).

[63] Yu YB. Fluorinated dendrimers as imaging agents for ^{19}F MRI. *WIREs Nanomed. Nanobiotechnol.* 5(6), 646–661 (2013).

[64] Hernández-Ainsa S, Barberá J. Fluorinated liquid crystalline dendrimers. *J. Fluor. Chem.* 177, 37–45 (2015).

[65] Liu X, Yuan Y, Bo S *et al.* Monitoring Fluorinated Dendrimer-Based Self-Assembled Drug-Delivery Systems with ^{19}F Magnetic Resonance. *Eur. J. Org. Chem.* 2017(30), 4461–4468 (2017).

[66] Moonshi SS, Zhang C, Peng H *et al.* A unique ^{19}F MRI agent for the tracking of non phagocytic cells in vivo. *Nanoscale.* 10(17), 8226–8239 (2018).

[67] Rolfe BE, Blakey I, Squires O *et al.* Multimodal Polymer Nanoparticles with Combined ^{19}F Magnetic Resonance and Optical Detection for Tunable, Targeted, Multimodal Imaging in Vivo. *J. Am. Chem. Soc.* 136(6), 2413–2419 (2014).

[68] Ogawa M, Nitahara S, Aoki H, Ito S, Narazaki M, Matsuda T. Fluorinated Polymer Nanoparticles as a Novel ^{19}F MRI Contrast Agent Prepared by Dendrimer-Initiated Living Radical Polymerization. *Macromol. Chem. Phys.* 211(12), 1369–1376 (2010).

[69] Srinivas M, Tel J, Schreibelt G *et al.* PLGA-encapsulated perfluorocarbon nanoparticles for simultaneous visualization of distinct cell populations by ^{19}F MRI. *Nanomedicine (Lond.)* 10(15), 2339–2348 (2015).

[70] Constantinides C, Basnett P, Lukasiewicz B *et al.* In Vivo Tracking and ^{1}H/^{19}F MRI of Biodegradable Polyhydroxyalkanoate/Polycaprolactone Blend Scaffolds Seeded with Labeled Cardiac Stem Cells.

ACS Appl. Mater. Interfaces 10(30), 25056–25068 (2018).

[71] Peterson KL, Srivastava K, Pierre VC. Fluorinated Paramagnetic Complexes: Sensitive and Responsive Probes for Magnetic Resonance Spectroscopy and Imaging. *Front Chem*. 6, 160 DOI: 10.3389/fchem.2018.00160 (2018).

[72] Knight JC, Edwards PG, Paisey SJ. Fluorinated contrast agents for magnetic resonance imaging; a review of recent developments. *RSC Adv.* 1, 1415–1425 (2011).

**** Review on the fluorinated contrast agents until 2011**

[73] Neubauer AM, Myerson J, Caruthers SD *et al.* Gadolinium-modulated ^{19}F signals from Perfluorocarbon Nanoparticles as a New Strategy for Molecular Imaging. *Magn. Reson. Med.* 60(5), 1066–1072 (2008).

[74] de Vries A, Moonen R, Yildirim M *et al.* Relaxometric studies of gadolinium-functionalized perfluorocarbon nanoparticles for MR imaging. *Contrast Media Mol. Imaging* 9(1), 83–91 (2014).

[75] Hitchens TK, Liu L, Foley LM, Simplaceanu V, Ahrens ET, Ho C. Combining Perfluorocarbon and Superparamagnetic Iron-Oxide Cell Labeling for Improved and Expanded Applications of Cellular MRI. *Magn. Reson. Med.* 73(1), 367–375 (2015).

[76] Kislukhin AA, Xu H, Adams SR, Narsinh KH, Tsien RY, Ahrens ET. Paramagnetic fluorinated nanoemulsions for sensitive cellular fluorine-19 magnetic resonance imaging. *Nat. Mater.* 15(6), 662–668 (2016).

[77] Senanayake PK, Kenwright AM, Parker D, van der Hoorn SK. Responsive fluorinated lanthanide probes for ^{19}F magnetic resonance spectroscopy. *Chem. Comm. (Camb.)* 28, 2923–2925 (2007).

[78] Schmid F, Höltke C, Parker D, Faber C. Boosting ^{19}F MRI—SNR Efficient Detection of Paramagnetic Contrast Agents Using Ultrafast Sequences. *Magn. Res. Med.* 69(4), 1056–1062 (2013).

[79] Chalmers KH, De Luca E, Hogg NHM *et al.* Design principles and theory of paramagnetic fluorine-labelled lanthanide complexes as probes for ^{19}F magnetic resonance: a proof-of-concept study. *Chem. - A Eur. J.* 16(1), 134–148 (2010).

[80] De Luca E, Harvey P, Chalmers KH *et al.* Characterisation and evaluation of paramagnetic fluorine labelled glycol chitosan conjugates for ^{19}F and ^{1}H magnetic resonance imaging. *J. Biol. Inorg. Chem.* 19(2), 215–227 (2014).

[81] Davies G-L, Brown A, Blackburn O *et al.* Ligation driven ^{19}F relaxation enhancement in self-assembled Ln(III) complexes. *Chem. Commun. (Camb.)* 51(14), 2918–2920 (2015).

[82] van Zijl PC, Yadav NN. Chemical Exchange Transfert (CEST): what is in a name and what isn't? *Magn. Reson. Med.* 65(4), 927–948 (2011).

[83] Schmieder AH, Caruthers SD, Keupp J, Wickline SA, Lanza GM. Recent Advances in ^{19}Fluorine

Magnetic Resonance Imaging with Perfluorocarbon Emulsions. *Engineering* 1(4), 475–489 (2015).

[84] Bar-Shir A, Yadav NN, Gilad AA, van Zijl PC, McMahon MT, Bulte JW. Single ^{19}F Probe for Simultaneous Detection of Multiple Metal Ions Using miCEST MRI. *J. Am. Chem. Soc*. 137(1), 78–81, 2015.

[85] Cakić N, Savić T, Stricker-Shaver J *et al.* Paramagnetic Lanthanide Chelates for Multicontrast MRI. *Chem. Comm. (Camb.)* 52(59), 9224–9227 (2016).

[86] Peng Q, Yuan Y, Zhang H *et al.* ^{19}F CEST imaging probes for metal ion detection. *Org. Biomol. Chem.* 15(30), 6441–6446 (2017).

[87] Mizukami S, Takikawa R, Sugihara F *et al.* Paramagnetic relaxation-based ^{19}F MRI probe to detect protease activity. J. *Am. Chem. Soc.* 130(3), 794–795 (2008).

[88] Mizukami S, Takikawa R, Sugihara F, Shirakawa M, Kikuchi K. Dual-Function Probe to Detect Protease Activity for Fluorescence Measurement and ^{19}F MRI. *Angew. Chem. Int. Ed. Engl.* 48(20), 3641–3643 (2009).

[89] Shalini S, Dorstyn L, Dawar S, Kumar S. Old, new and emerging functions of caspases. *Cell Death Differ.* 22(4), 526–539 (2014).

[90] Yuan Y, Sun H, Ge S *et al.* Controlled Intracellular Self-Assembly and Disassembly of 19F Nanoparticles for MR Imaging of Caspase 3/7 in Zebrafish. *ACS Nano.* 9(1), 761–768 (2015).

[91] Yuan Y, Ge S, Sun H *et al.* Intracellular Self-Assembly and Disassembly of ^{19}F Nanoparticles Confer Respective "Off" and "On" ^{19}F NMR/MRI Signals for Legumain Activity Detection in Zebrafish. *ACS Nano.* 9(5), 5117–5124 (2015).

[92] Ekanger LA, Mills DR, Ali MM *et al.* Spectroscopic Characterization of the 3+ and 2+ Oxidation States of Europium in a Macrocyclic Tetraglycinate Complex. *Inorg. Chem.* 55(20), 9981–9988 (2016).

[93] Oishi M, Sumitani S, Nagasaki Y. On-Off Regulation of 19F Magnetic Resonance Signals Based on pH-Sensitive PEGylated Nanogels for Potential Tumor-Specific Smart ^{19}F MRI Probes. *Bioconj. Chem.* 18(5), 1379–1382 (2007).

[94] Wang K, Peng H, Thurecht KJ, Puttick S, Whittaker AK. pH-responsive star polymer nanoparticles: potential ^{19}F MRI contrast agents for tumour-selective imaging. *Polym. Chem.* 4, 4480–4489 (2013).

[95] Iima R, Takegami S, Konishi SA, Tajima S, Minematsu N, Kitade T. Thermal Behavior of ^{19}F Nuclear Magnetic Resonance Signal of ^{19}F-Containing Compound in Lipid Nano-Emulsion for Potential Tumor Diagnosis. *AAPS PharmSciTech* 19(6), 2679–2686 (2018).

[96] Langereis S, Keupp J, van Velthoven JL *et al*. A Temperature-Sensitive Liposomal ^{1}H CEST and ^{19}F Contrast Agent for MR Image-Guided Drug Delivery. *J. Am. Chem. Soc.* 131(4), 1380–1381

(2009).

[97] Kolouchova K, Sedlacek O, Jirak D *et al.* Self-assembled Thermoresponsive Polymeric Nanogels for ^{19}F MR Imaging. *Biomacromolecules* 19(8), 3515–3524 (2018).

[98] Bober Z, Aebisher D, Ożóg L, Tabarkiewicz J, Tutka P, Bartusik-Aebisher D. ^{19}F MRI As a tool for imaging drug delivery to tissue and individual cells. *Eur. J. Clin. Exp. Med.* 15(2), 109–119 (2017).

[99] Seitz JD, Vineberg JG, Wei L *et al.* Design, synthesis and application of fluorine-labeled taxoids as ^{19}F NMR probes for the metabolic stability assessment of tumor-targeted drug delivery systems. *J. Fluor. Chem.* 171, 148–161 (2015).

[100] Vu-Quang H, Vinding MS, Nielsen T, Ullisch MG, Nielsen NC, Kjems J. Theranostic tumor targeted nanoparticles combining drug delivery with dual near infrared and ^{19}F magnetic resonance imaging modalities. *Nanomedicine* 12(7), 1873–1884 (2016).

[101] Bo S, Yuan Y, Chen Y *et al.* In vivo Drug Tracking with ^{19}F MRI at Therapeutic Dose. *Chem. Comm. (Camb.)* 54(31), 3875–3878 (2018).

[102] Fox MS, Gaudet JM, Foster PJ. Fluorine-19 MRI Contrast Agents for Cell Tracking and Lung Imaging. *Magn. Reson. Insights* 8(S1), 53–67 (2016).

[103] Ahrens ET, Flores R, Xu H, Morel PA. In vivo imaging platform for tracking immunotherapeutic cells. *Nat. Biotechnol.* 23(8), 983–987 (2005).

*** One of the first publication on ^{19}F MRI cell tracking**

[104] Helfer B, Balducci A, Nelson AD *et al.* Functional assessment of human dendritic cells labeled for in vivo ^{19}F magnetic resonance imaging cell tracking. *Cytotherapy* 12(2), 238–250 (2010).

[105] Ahrens ET, Zhong J. In vivo MRI cell tracking using perfluorocarbon probes and fluorine-19 detection. *NMR Biomed.* 26(7), 860–871 (2013).

[106] Ahrens ET, Helfer BM, O'Hanlon CF, Schirda C. Clinical cell therapy imaging using a perfluorocarbon tracer and fluorine-19 MRI. *Magn. Reson. Med.* 72(6), 1696–1701 (2014).

[107] Gaudet JM, Ribot EJ, Chen Y, Gilbert KM, Foster PJ. Tracking the Fate of Stem Cell Implants with Fluorine-19 MRI. *PLoS One* 10(3), e0118544 DOI: 10.1371/journal.pone.0118544 (2015).

[108] Srinivas M, Morel PA, Ernst LA, Laidlaw DH, Ahrens ET. Fluorine-19 MRI for Visualization and Quantification of Cell Migration in a Diabetes Model. *Magn. Reson. Med.* 58(4), 725–734 (2007).

[109] Balducci A, Helfer BM, Ahrens ET, O'Hanlon CF 3rd, Wesa AK. Visualizing arthritic inflammation and therapeutic response by fluorine-19 magnetic resonance imaging (^{19}F MRI). *J. Inflamm. (Lond.)* 9(1), 24 (2012).

[110] Weibel S, Basse-Luesebrink TC, Hess M *et al.* Imaging of Intratumoral Inflammation during

Oncolytic Virotherapy of Tumors by ^{19}F-Magnetic Resonance Imaging (MRI). *PLoS One* 8(2), e56317 DOI: 10.1371/journal.pone.0056317 (2013).

[111] Balducci A, Wen Y, Zhang Y *et al.* A novel probe for the non-invasive detection of tumor-associated inflammation. *Oncoimmunology* 2(2), e23034 (2013).

[112] Ebner B, Behm P, Jacoby C *et al.* Early Assessment of Pulmonary Inflammation by ^{19}F MRI In Vivo. *Circ. Cardiovasc. Imaging* 3(2), 202–210 (2010).

[113] Jacoby C, Borg N, Heusch P *et al.* Visualization of immune cell infiltration in experimental viral myocarditis by ^{19}F MRI in vivo. *Magn. Reson. Mater. Phy. MAGMA* 27(1), 101–106 (2013).

[114] Bönner F, Merx MW, Klingel K *et al.* Monocyte imaging after myocardial infarction with ^{19}F MRI at 3 T: a pilot study in explanted porcine hearts. *Eur. Heart J. Cardiovasc. Imaging* 16(6), 612–620 (2015).

[115] Flögel U, Su S, Kreideweiss I *et al.* Noninvasive Detection of Graft Rejection by In Vivo (19) F MRI in the Early Stage. *Am. J. Transplant.* 11(2), 235–244 (2011).

[116] Hitchens TK, Ye Q, Eytan DF, Janjic JM, Ahrens ET, Ho C. 19F MRI Detection of Acute Allograft Rejection with In Vivo Perfluorocarbon Labeling of Immune Cells. *Magn. Reson. Med.* 65(4), 1144–1153 (2011).

[117] Gaudet JM, Hamilton AM, Chen Y, Fox MS, Foster PJ. Application of Dual ^{19}F and Iron Cellular MRI Agents to Track the Infiltration of Immune Cells to the Site of a Rejected Stem Cell Transplant. *Magn. Reson. Med.* 78(2), 713–720 (2017).

[118] Shin SH, Park EJ, Min C *et al*. Tracking Perfluorocarbon Nanoemulsion Delivery by ^{19}F MRI for Precise High Intensity Focused Ultrasound Tumor Ablation. *Theranostics.* 7(3), 562–572 (2017).

[119] Makela AV, Gaudet JM, Foster PJ. Quantifying tumor associated macrophages in breast cancer: a comparison of iron and fluorine-based MRI cell tracking. *Sci. Rep.* 7, 42109 DOI: 10.1038/srep42109 (2017).

[120] Khurana A, Chapelin F, Xu H *et al.* Visualization of Macrophage Recruitment in Head and Neck Carcinoma Model Using Fluorine-19 Magnetic Resonance Imaging. *Magn. Reson. Med.* 79(4), 1972–1980 (2018).

[121] Makela AV, Foster PJ. Imaging Macrophage Distribution and Density in Mammary Tumors and Lung Metastases Using Fluorine-19 MRI Cell Tracking. *Magn. Reson. Med.* 80(3), 1138–1147 (2018).

[122] Shin SH, Park SH, Kang SH, Kim SW, Kim M, Kim D. Fluorine-19 Magnetic Resonance Imaging and Positron Emission Tomography of Tumor-Associated Macrophages and Tumor Metabolism. *Contrast Media Mol. Imaging* 2017, 4896310 DOI: 10.1155/2017/4896310 (2017).

[123] Fink C, Gaudet JM, Fox MS *et al.* ^{19}F-perfluorocarbon-labeled human peripheral blood

mononuclear cells can be detected in vivo using clinical MRI parameters in a therapeutic cell setting. *Sci. Rep.* 8(1), 590 DOI: 10.1038/s41598-017-19031-0 (2018).

[124] Bo S, Song C, Li Y *et al.* Design and Synthesis of Fluorinated Amphiphile as ^{19}F MRI/ Fluorescence Dual-Imaging Agent by Tuning the Self-Assembly. *J. Org. Chem.* 80(12), 6360–6366 (2015).

[125] Peng Q, Li Y, Bo S *et al.* Paramagnetic nanoemulsions with unified signal for sensitive ^{19}F MRI cell tracking. *Chem. Comm. (Camb.)* 54(47), 6000–6003 (2018).

[126] Temme S, Jacoby C, Ding Z *et al.* Technical advance: monitoring the trafficking of neutrophil granulocytes and monocytes during the course of tissue inflammation by noninvasive ^{19}F MRI. *J. Leukoc. Biol.* 95(4), 689–697 (2014).

[127] Jacoby C, Temme S, Mayenfels F *et al.* Probing different perfluorocarbons for in vivo inflammation imaging by ^{19}F MRI: Image reconstruction, biological half-lives and sensitivity. *NMR Biomed.* 27(3), 261–271 (2014).

[128] Colotti R, Bastiaansen JA, Wilson A *et al.* Characterization of Perfluorocarbon Relaxation Times and their Influence on the Optimization of Fluorine-19 MRI at 3 Tesla. *Magn Reson Med* 77(6), 2263–2271 (2016).

[129] van Heeswijk RB, Pellegrin M, Flögel U *et al.* Fluorine MR Imaging of Inflammation in Atherosclerotic plaque in vivo. *Radiology* 275(2), 421–429 (2015).

[130] Moyer LC, Timbie KF, Sheeran PS, Price RJ, Miller GW, Dayton PA. High-intensity focused ultrasound ablation enhancement in vivo via phase-shift nanodroplets compared to microbubbles. *J. Ther. Ultrasound* 3, 7 DOI: 10.1186/s40349-015-0029-4 (2015).

[131] Moyer L, Timbie K, Sheeran P, Price R, Miller W, Dayton P. Direct nanodroplet and microbubble comparison for high intensity focused ultrasound ablation enhancement and safety. *J. Ther. Ultrasound* 3(S1), DOI: 10.1186/2050-5736-3-S1-067 (2015).

[132] Shin SH, Park SH, Kim SW, Kim M, Kim D. Fluorine MR Imaging Monitoring of Tumor Inflammation after High-Intensity Focused Ultrasound Ablation. *Radiology* 287(2), 476–484 (2018).

[133] Wu L, Wen X, Wang X *et al.* Local Intratracheal Delivery of Perfluorocarbon Nanoparticles to Lung Cancer Demonstrated with Magnetic Resonance Multimodal Imaging. *Theranostics.* 8(2), 563–574 (2018).

- **Reference annotations**: authors should highlight 6–8 references that are of particular significance to the subject under discussion as **"* of interest"** or **"** of considerable interest"**, and provide a brief (1–2 line) synopsis.

Modality	Spatial resolution	Depth	Advantages	Inconvenient
CT	50-200 mm	No limit	High spatial resolution	Radiation, poor tissue imaging
MRI	0.01-0.1 mm	No limit	High spatial resolution, excellent signal in soft tissues, no ionizing radiation	Targeted imaging tracer availability, low sensitivity
US	50-500 mm	mm-cm	Relatively good spatial and temporal resolution, safety	Low sensitivity
OI	1-5 mm	mm	High sensitivity, no radiation exposure, high throughput	Poor tissue penetration, low resolution
PET / SPECT	0.5-2 mm	No limit	Good sensitivity, dynamic	Targeted imaging tracer availability, radiation, low spatial resolution

Linear GBCAs

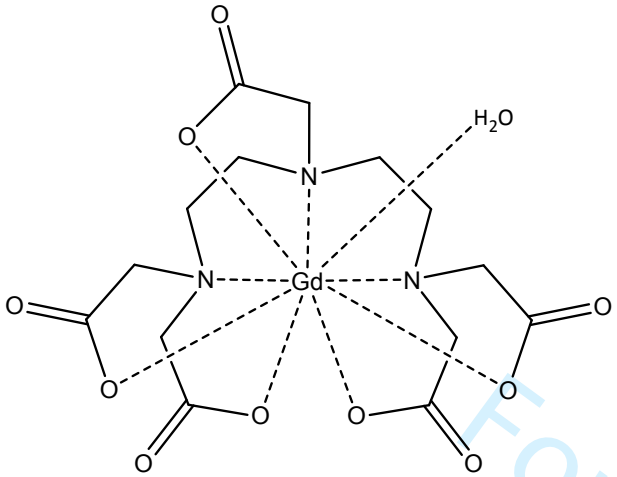

MAGNEVIST ® (Gd-DTPA)

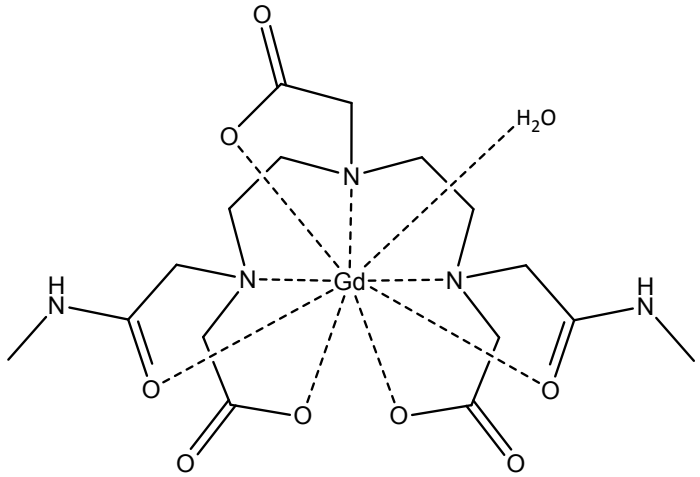

OMNISCAN ® (Gd(DTPA-BMA))

Macrocyclic GBCAs

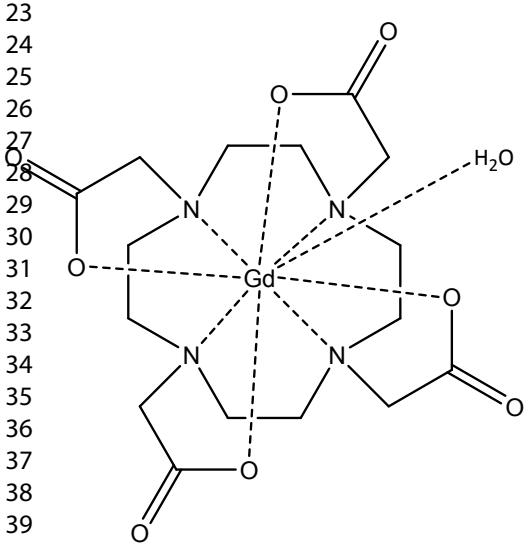

DOTAREM ® (Gd-DOTA)

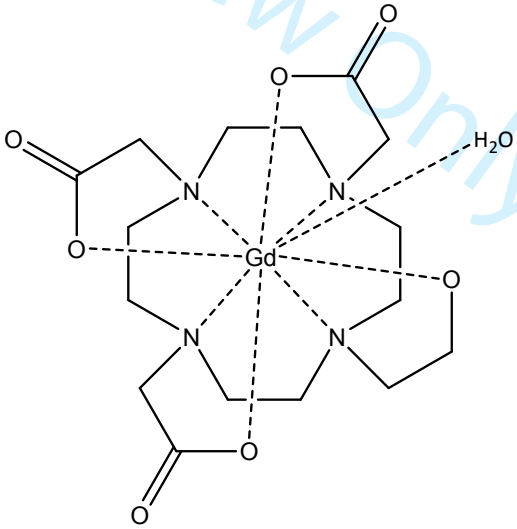

Prohance ® (Gd(HP-DO3A))

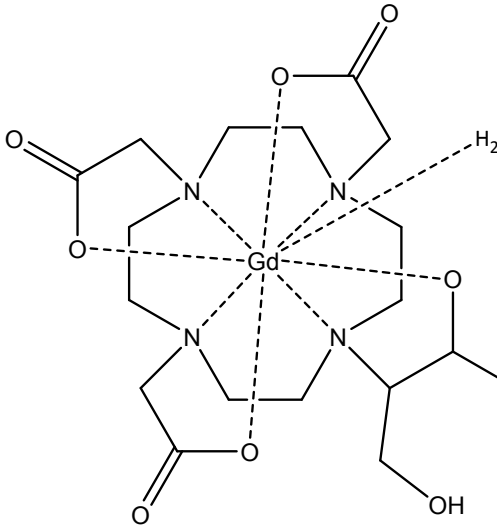

Gadovist ® (Gd(DO3A-butrol))

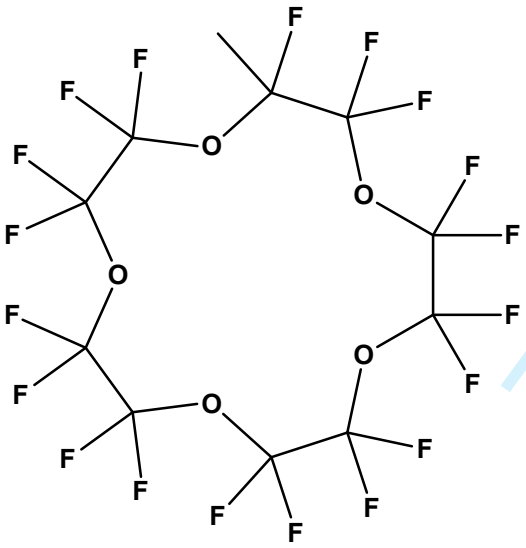

Perfluoro-15-crown-5 ether (PFCE)

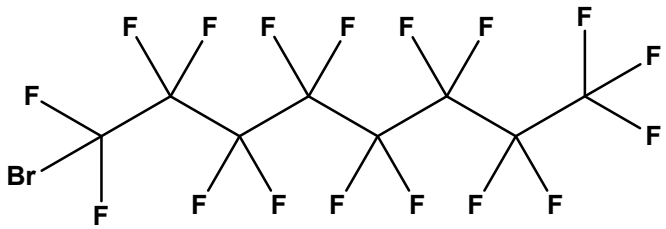

Perfluorooctyl bromide (PFOB)

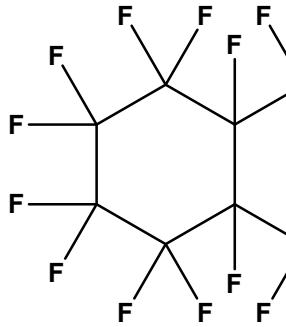

Perfluorodec

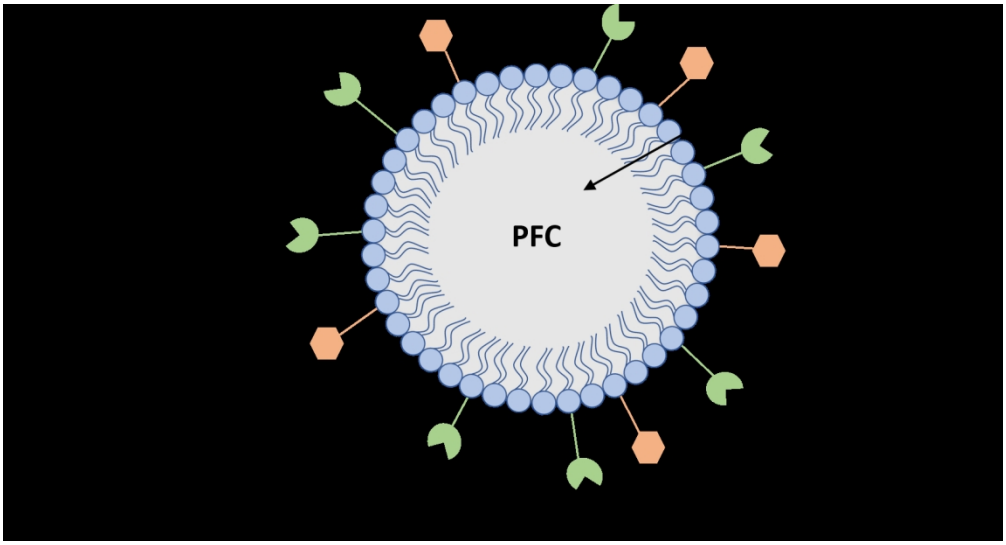

Scheme of PFC nanoemulsions containing perfluorocarbonated core within a lipid monolayer on which payloads and targeting ligands can be linked.

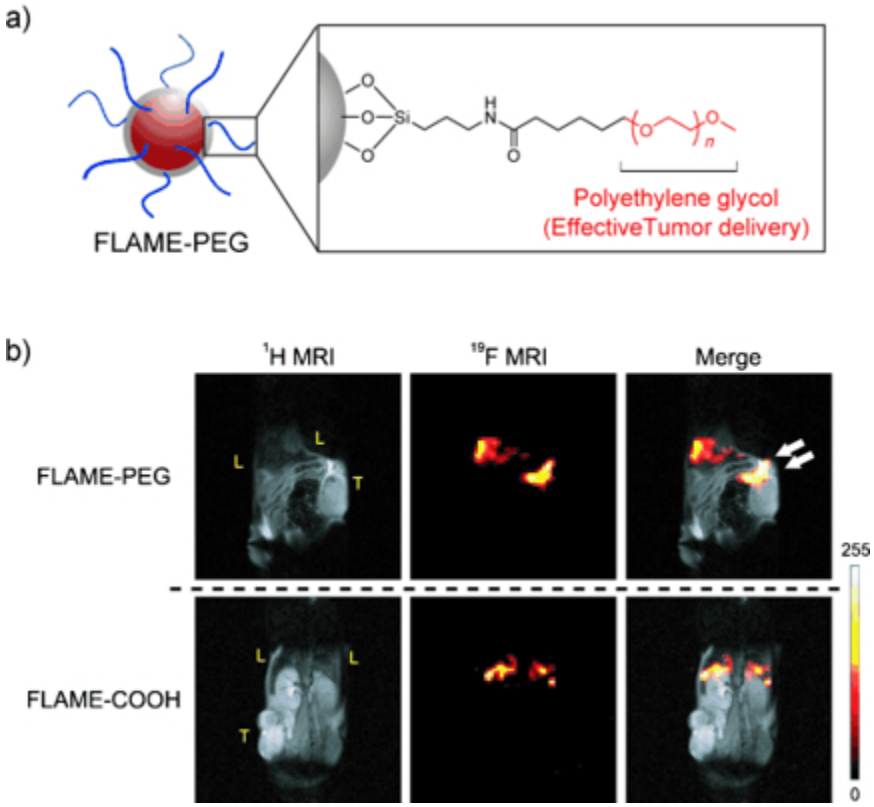

In vivo distribution of FLAME at tumorous site. (a) Structure of PEGylated FLAME (b) In vivo images of the accumulation of FLAME PEGylated (FLAME-PEG) and non-PEGylated (FLAME-COOH) in tumor-bearing mice. The superimposition of 1H and 19F MRI images shows the difference between the distribution of FLAMEs in liver (L) and tumor (T) (Reprinted with permission from Matsushita H, Mizukami S, Sugihara F, Nakanishi Y, Yoshioka Y, Kikuchi K. Multifunctional Core–Shell Silica Nanoparticles for Highly Sensitive 19F Magnetic Resonance Imaging, Volume: 53, Issue: 4, Pages: 1008-1011, First published: 20 January 2014, DOI: (10.1002/anie.201308500) [55])

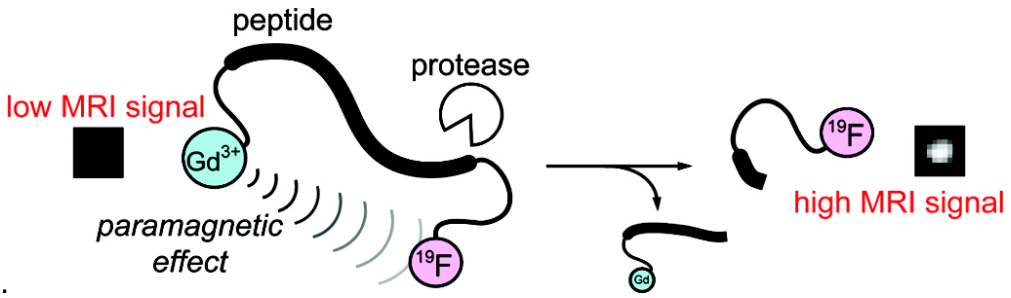

Scheme of enzyme-responsive fluorinated agent to detect caspase-3 activity. (Reprinted with permission from Mizukami S, Takikawa R, Sugihara F et al. Paramagnetic relaxation-based 19F MRI probe to detect protease activity. Copyright 2008 American Chemical Society [87])

361x103mm (72 x 72 DPI)